Optics & Laser Technology 52 (2013) 15–20

Contents lists available at SciVerse ScienceDirect

Optics & Laser Technology

journal homepage: www.elsevier.com/locate/optlastec

# High gain pulsed erbium-doped fiber amplifier for the nonlinear characterization of SWCNTs photodeposited on optical fibers

P. Zaca-Morán [a], E. Kuzin [b], J. Torres-Turiján [c], J.G. Ortega-Mendoza [d], F. Chávez [a], G.F. Pérez-Sánchez [a], L.C. Gómez-Pavón [c,*]

[a] Departamento de Fisicoquímica de Materiales, ICUAP-BUAP, C.P. 72050 Puebla, Mexico
[b] Instituto Nacional de Astrofísica, Óptica y Electrónica, INAOE, C.P. 72000 Puebla, Mexico
[c] Facultad de Ciencias de la Electrónica, BUAP, San Claudio y 18 Sur, Edif. 109B, San Manuel, C.P. 72570 Puebla, Mexico
[d] Facultad de Ciencias Físico Matemáticas, BUAP, San Claudio y Río Verde, San Manuel, C.P. 72570 Puebla, Mexico

ARTICLE INFO

*Article history:*
Received 2 January 2013
Received in revised form
29 March 2013
Accepted 2 April 2013
Available online 3 May 2013

*Keywords:*
Optical amplifier
High gain
Nonlinear characterization

ABSTRACT

We report the experimental setup of a high power pulsed erbium-doped fiber amplifier. An optical signal at 1550 nm emitted by a distributed feedback laser is amplified by two identical stages in reflective configuration using one fiber Bragg grating at each one of those. We demonstrated that for pulses with a frequency of 20 kHz and temporal duration of 10, 50, 100, and 500 ns, it is possible to obtain output peak powers of 41, 22, 18, and 11 W, respectively. We applied our high power amplifier in the characterization of nonlinear optical transmission of single-wall carbon nanotubes deposited on single mode optical fibers end-face by the photodeposition technique. Our results show that the high power system is ideal for carrying out studies of nonlinear effects in optical fibers as well as nonlinear characterization of nanostructured materials deposited on optical fibers.


## 1. Introduction

There is a growing demand for pulsed lasers operating in the infrared region for use in several industrial fields including high-speed communications, signal processing and optical metrology. Currently, the third window of optical communications at 1550 nm has been the best option for simultaneous transmission over long distances of multiplexed signals. The result is the development of devices that recover and amplify the signal for retransmission [1]. Particularly, in this region the erbium-doped fiber amplifiers (EDFA) are widely used as a gain medium and have been in continuous development [2,3].

An optical amplifier whose excited carriers amplify an incident signal is a device that amplifies an optical signal directly operating on similar to those the laser, but without feedback. The amplification mechanism is made by stimulated emission through pumping to carry out the population inversion that depends not only on the frequency of the incident signal, but also on the local beam intensity at any point of the amplifier.

In the pulsed regime, the extractable energy is strongly limited by nonlinear effects (specially stimulated Brillouin scattering, SBS) and unwanted amplified spontaneous emission (ASE), which lead to fast self-saturation. In such a system, when the amplifier energy reaches the saturation level the output pulse will be distorted. The leading edge of the pulse will get a high gain depleting the population inversion, so the rest of the pulse will decrease exponentially. Moreover, the build-up of amplified spontaneous emission (ASE) between pulses limits the output pulse energy. To address these issues, a judicious selection of pulse duration ($t$) and repetition rate ($f$) are required.

Bello-Jimenez et al. developed an EDFA with two-stages amplification using a single pump for both of them. To reduce the ASE a Sagnac interferometer was proposed. The experimental results demonstrated an amplification of up to 53 dB with 73 mW of pump power. However, the disadvantage of this arrangement is that the output power depends on the polarization in the Sagnac interferometer. Therefore, the system requires constant adjustments for maximum transmission and as a consequence maximum output power [4].

Camas et al. developed a two-stage EDFA. The reflective configuration design of the first stage was performed with a Bragg grating that allows the reflection of the signal being amplified twice. This stage works as a high gain amplifier and a second stage as a high power amplifier. The authors reported an amplified signal obtaining a maximum peak power of 70 W. The disadvantage of this experimental setup is that the output signal does not include a filtering system to reduce the ASE levels [5].

On the other hand, the single wall carbon nanotubes (SWCNTs) have interesting nonlinear optical properties, such as saturable

* Corresponding author. Tel.: +52 222 229 5500.
*E-mail addresses:* placido.zaca@correo.buap.mx (P. Zaca-Morán), luz.gomez@correo.buap.mx (L.C. Gómez-Pavón).

0030-3992 
http://dx.doi.org/10.1016/j.optlastec.2013.04.004

absorbers, because its absorption peak is in the infrared region, and because of the dependence between the bandgap with both morphological, and structural properties [6–10]. In the third window of optical communications, the SWCNTs have potential applications, including optical switching, passive mode locking and noise suppression in transmission systems [11–14].

The nonlinear characterization techniques of those nanostructures mostly depend on the form that are analyzed: on a substrate, diluted in a solution, or directly deposited on a fiber optic connector [15,16]. It is noteworthy that the presence of additional components may increase the level of losses, resulting in an unsaturated optical absorption, thus decreasing the efficiency of the nonlinear optical element.

Il'ichev et al. performed the nonlinear characterization of SWCNTs with a pulsed laser of 40 MW $cm^{-2}$ at 1540 nm. The fact that the SWCNTs were in a cell with a solution of $D_2O$ complicated the characterization. The nonlinear effects in both the cell and solution must not be discriminated [13].

Kivistö et al. reported the nonlinear characterization of SWCNTs deposited on a silver mirror, and a modulation depth lower than 1% was obtained as a result. The characterization was performed by a source of short pulses with an active media of both erbium and ytterbium, which implies an expensive system [12].

In this paper, we present the experimental development of a high power dual-stage amplifier for nonlinear characterization of SWCNTs photodeposited on optical fiber end-face. Each amplification stage uses reflective Bragg gratings and the input signal is amplified four times. Among the advantages of our system are that in both stages of amplification use a semiconductor laser only; the signal amplification is adjustable by means of both the frequency of the laser signal as well as the temporal output pulse duration.

## 2. High gain laser implementation

In Fig. 1, we present the first stage of amplification in reflective configuration. This stage consists of a distributed feedback laser (DFB) at 1550 nm, 10-m-long single-mode Er-doped fiber (EDF) as a gain medium, and a three port optical circulator (OC1), where the pulsed signal at 1550 nm is input to port 1 and sent to EDF through port 2. The pumping power is coupled into the EDF by means of 980/1550-nm wavelength division multiplexing (WDM-1) coupler. Finally, a fiber Bragg grating (FBG) with 99% of reflection at 1550 nm is coupled to the WDM-1 as a filter.

The pulses characteristics from the DFB laser are controlled by three systems: a temperature controller to stabilize the wavelength of operation, a current source to adjust the output power level and, a pulse generator to program both the frequency as well as the temporal pulses duration. We performed the DFB laser characterization through the variation of current and temperature drivers. The current was set from 0 up to 14.5 mA, and the temperature from 5 up to 35 °C.

Fig. 2 shows the output power of the DFB laser as a function of the current applied at different temperatures. The laser output power presents a linear behavior regarding to current applied. Furthermore, the temperature increase leads to decrease in power as well as increasing in current threshold.

We measured the emission spectrum of the DFB laser at 25 °C. The pulse generator was set at 20 kHz with temporal pulses of 50 ns. In Fig. 3, we present the spectrum with a full-width at half-maximum (FWHM) of 0.2 nm with a center line approximately at 1550 nm.

In Fig. 4, we observe the results of the sensitivity characterization of the InGaAs photodetector. The voltage regarding the laser output power presents a linear behavior. Taking into account the data distribution and considering that it is possible to extract the sensitivity from the slope of the voltage vs. output power dependence, the sensitivity is 45.2 mV/mW, approximately.

The experimental configuration of the second stage of amplification in the high power amplifier is similar to the first stage. The amplified signal from the first stage output through port 3 of first optical circulator, OC1, is input to the second stage through port 1 of second optical circulator, OC2. The pump source at 980 nm for active media in both stages of amplification is a semiconductor laser only, which is coupled by means of a 70/30 coupler. Finally, to adjust the output power from the high power amplifier, port 3 of OC2 is connected to the setup for output power control. Such control is performed by an attenuator, as it is shown in Fig. 5.

With the aim to demonstrate an application of high power amplification system developed, we performed the nonlinear characterization of SWCNTs photodeposited on the optical fiber end-face.

The photodeposition technique has been studied by Ortega-Mendoza et al. In Fig. 6, we show the experimental setup of photodeposition technique, which is performed propagating cw laser radiation at 980 nm throughout an optical fiber, and the end-face of cleaved optical fiber is introduced in a solution with isopropyl alcohol, where the SWCNTs have previously been mixed [17].

The output radiation from the optical fiber end-face is able to affect the dynamics of SWCNTs in the solution, such that these are attracted to regions where the radiation intensity is greater. As a consequence the SWCNTs are deposited mainly on the core of the optical fiber end-face. In this work, we have used nanotubes manufactured by catalytic CVD method. Fig. 7 shows the SEM image of SWCNTs deposited on the optical fiber end-face.

We applied the high power amplification system to obtain a high power pulsed laser that allows to achieve the nonlinear characterization of SWCNTs photodeposited.

As we show in Fig. 8, a 90/10 coupler is fused with the output of high power amplification system. About 90% of radiation intensity

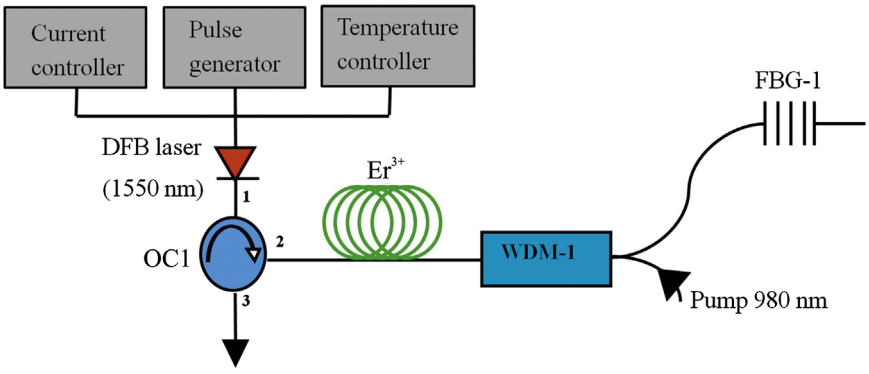


**Fig. 1.** Experimental setup of the first amplification stage.

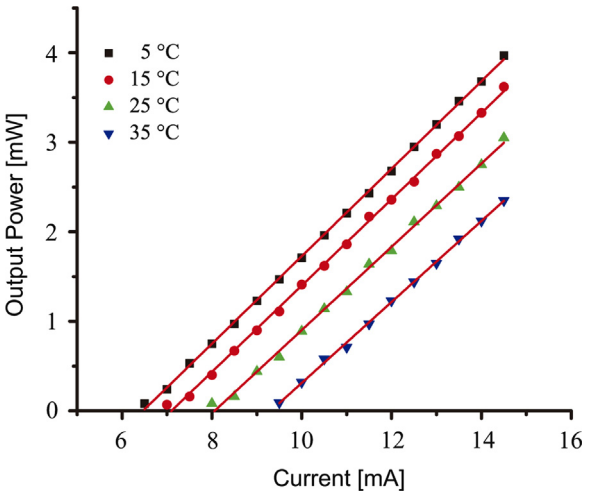


**Fig. 2.** Output power of the DFB laser versus bias current drive at different temperatures.

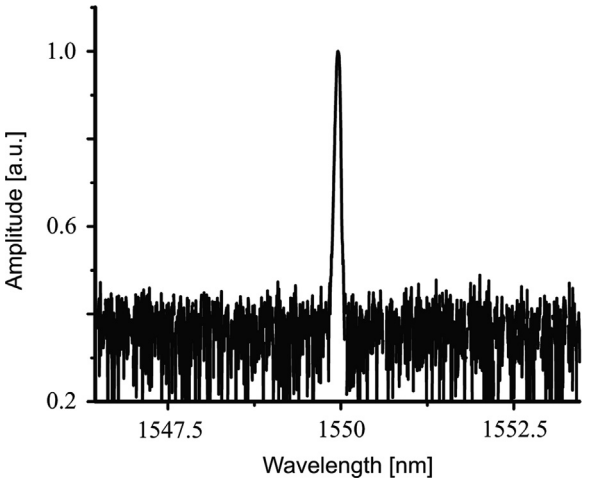


**Fig. 3.** Emission spectrum of the DFB laser.

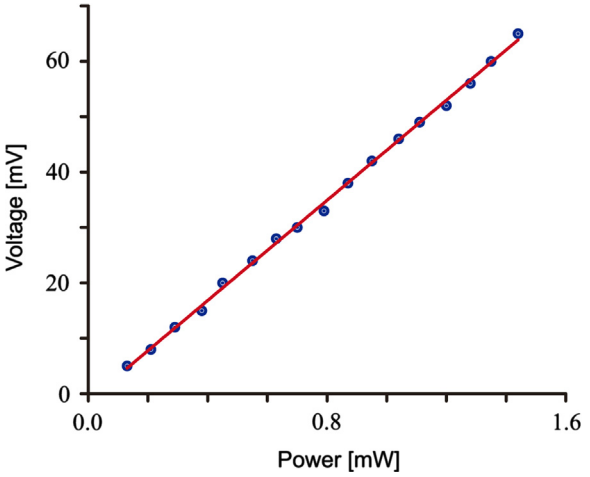


**Fig. 4.** Photodetector sensitivity. Voltage regarding the DFB output power laser.

is coupled to the optical fiber input with SWCNTs deposited at the end of it. We obtain the nonlinear optical transmission of SWCNTs by the ratio between the output power and the power that was measured at the 90% of the coupler prior to fusion.

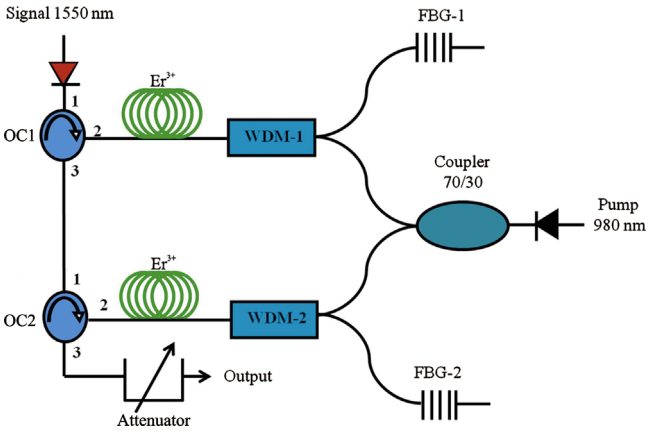


**Fig. 5.** Experimental setup of high power erbium-doped fiber amplifier.

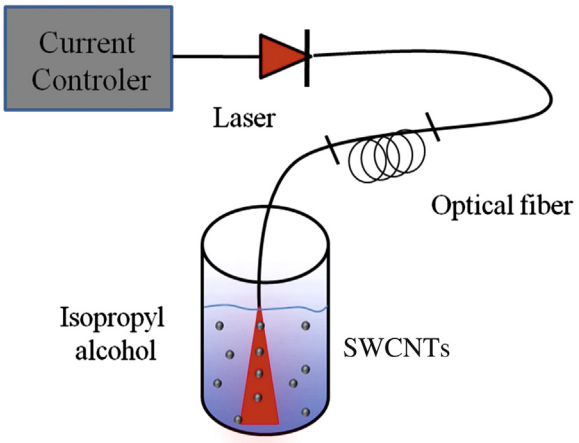


**Fig. 6.** Experimental setup for photodeposition process of SWCNTs on the optical fiber end-face.

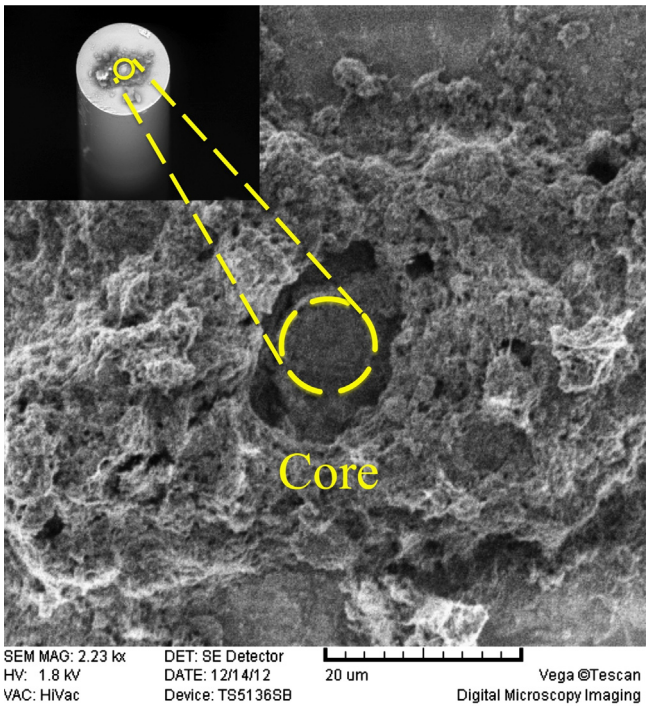


**Fig. 7.** SEM image of SWCNTs deposited on the optical fiber end-face by photo-deposition technique.

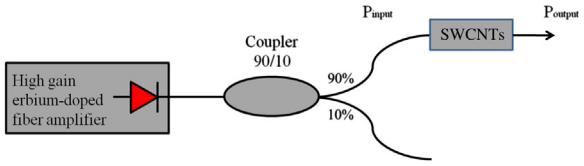


**Fig. 8.** Experimental setup for nonlinear characterization of SWCNTs deposited on the optical fiber end-face.

In this case the SWCNTs sample is fixed on the optical fiber end-face, and the incident intensity on the sample is varied. The transmission at the sample can be expressed as a function of the intensity using the Beer–Lambert law [18]

$$T = \exp[-(\alpha_0 + \beta I)L], \tag{1}$$

where $\alpha_0$ and $\beta$ are the lineal and nonlinear absorption coefficient, respectively, $L$ is the sample length, and $I$ is the intensity. We considered a saturation model and therefore, we used a hyperbolic approximation [19]

$$\beta(I) = \frac{\beta_0}{1 + I/I_{sat}}, \tag{2}$$

where $I_{sat}$ the saturation intensity is defined as the intensity when the transmission has reached 50% of depth of modulation.

By combining Eqs. (1) and (2) we obtained the transmittance expression as

$$T = \exp\left[-\left(\alpha_0 + \frac{\beta_0 I}{1 + I/I_{sat}}\right)L\right] \tag{3}$$

## 3. Results

The characterization of the first stage of amplification is performed with the pulse generator of the DFB laser programmed at 20 kHz of frequency. The temporal output pulses are of 10, 50, 100, and 500 ns with a maximum peak power of 3.4, 1.5, 0.80, and 0.28 W, respectively, as it is shown in Fig. 9. In this figure, we observe that the output power is inversely proportional to the temporal pulse duration, i.e. for shorter pulses the power is increased. Such behavior allows to have an adjustable output power through the temporal duration of the pulses.

In Fig. 10, we show the characterization results of the second stage of amplification. In this case, taking into account the aforementioned temporal pulses, we obtained maximum peak powers of 41, 22, 18 and 11 W. Therefore, the maximum gain obtained is 43.10 dB with laser pulses of 10 ns at 20 kHz and maximum peak power of 41 W. We have observed that at lower frequency, 1 kHz, and temporal pulse duration of 10 ns, it is possible to obtain an output peak power greater than 150 W.

Fig. 11(a) shows the high power laser spectrum, the peak intensity is observed at 1550 nm, approximately. In Fig. 11(b), we present the output spectrum for each one of the temporal pulses around the peak intensity at 1550 nm. We observed that as the temporal pulses duration are reduced, the spectral width is wider, and such behavior is consistent with the Fourier transform.

In Fig. 12, we present the temporal output pulses of 10, 50, 100, and 500 ns. We observe that the decay of the pulses is proportional to the pulse duration, i.e. the decay is greater for pulses of 100 and 500 ns in comparison with pulses of 10 and 50 ns. We consider that such behavior is because the high power amplifier is working in the saturation region. The pulse intensity is high enough to induce a high stimulated emission in the amplifier and consequently, the pumping is no longer able to maintain a high population inversion.

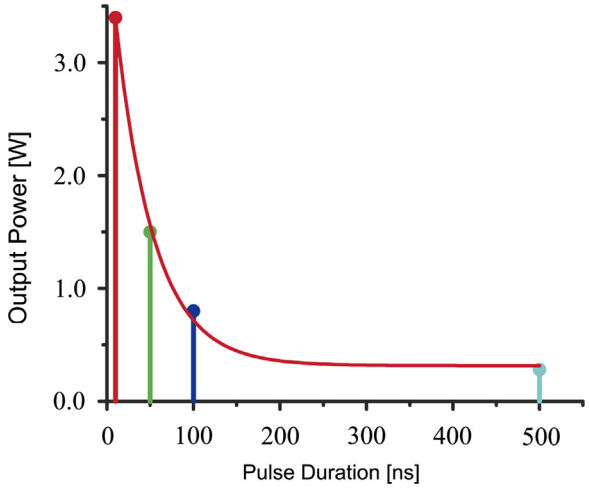


**Fig. 9.** Output power in function of the temporal pulses duration for the first amplifier stage.

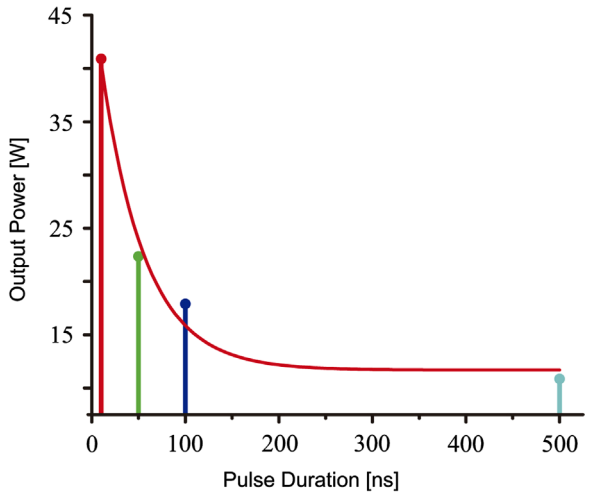


**Fig. 10.** Output power in function of the temporal pulses duration for the high power erbium-doped amplifier.

An advantage of using a two-stage amplifier in reflective configuration is that in each stage the signal is amplified twice. The Bragg grating placed at the end of each stage has a dual function. First, it performs a process of signal filtering, and second it operates in reflection mode at a specified wavelength, which makes that the selected signal passes a second time through the active medium, and the signal is amplified again. Therefore, the signal is amplified four times through all the experimental setup. Moreover, our amplifier uses a single pumping source for two amplifier stages. This characteristic allows us to consider the high power optical fiber amplifier developed both a simpler and inexpensive system, in comparison with other ones that have pump sources for each stage.

To demonstrate an application of the high power amplifier, we achieved the nonlinear characterization of SWCNTs photodeposited on optical fibers end-face. In this case, it was necessary to take into account that due to the incident radiation power increases, the deposited nanotubes can be detached from the optical fiber end-face. In this case, to prevent the SWCNTs detachment, a layer of nitrocellulose-based lacquer was placed. Therefore, with the aim of eliminating the possibility that the lacquer can contribute to the nonlinear effects, the nonlinear characterization was achieved without SWCNTs deposited on the optical fiber end-face. In Fig. 13, it is observed that the lacquer applied has a linear

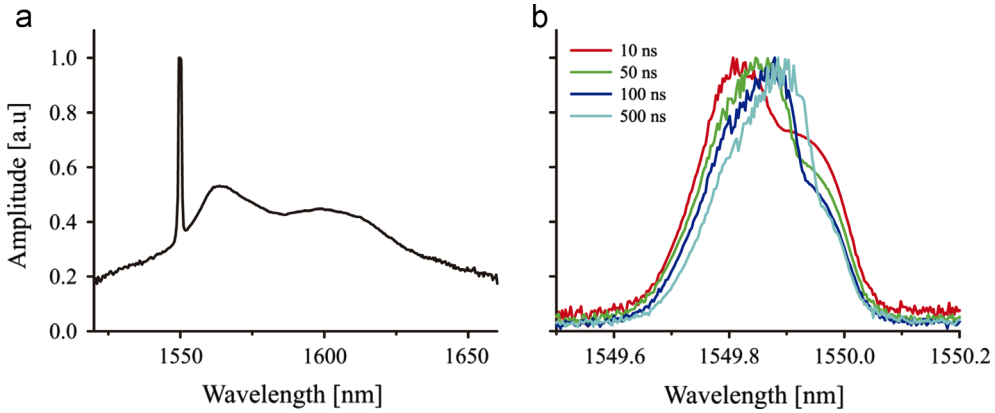


**Fig. 11.** (a) Spectrum of the high power pulse amplifier. (b) Emission spectra of the amplified pulses of 10, 50, 100, and 500 ns.

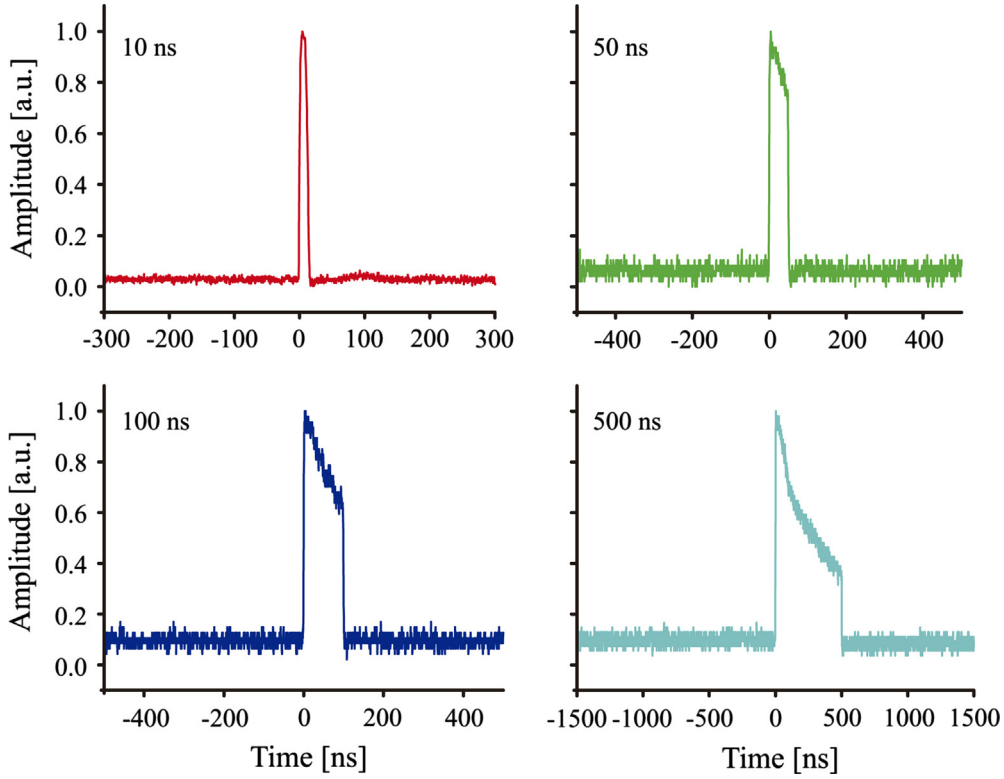


**Fig. 12.** Output pulses of 10, 50, 100, and 500 ns from the high power amplifier.

transmission for incident intensities of up to $3.8 \times 10^8$ W/cm$^2$ from the high-gain amplifier developed.

The nonlinear characterization of SWCNTs deposited on the optical fiber end-face is performed applying intensities of up to $2.4 \times 10^8$ W/cm$^2$ from the high-gain erbium-doped fiber amplifier. The results are shown in Fig. 14, the inset presents the transmission behavior at lower incident intensities, it is observed that the nonlinear effects of SWCNTs start at $0.5 \times 10^7$ W/cm$^2$, approximately. Since such input intensity is observed up to 60% of nonlinear transmission of the SWCNTs, the saturation is obtained at around $2.4 \times 10^8$ W/cm$^2$ of incident intensity.

The curve fitting in Fig. 14 was obtained using Eq. (3), with $\beta_0 = -2.47 \times 10^{-6}$ m/W, and $\chi_{3img} \approx 4.31 \times 10^{-14}$ m$^2$/V$^2$ ($\approx 3.08 \times 10^{-6}$ esu). In the inset, for lower intensities, $\beta_0 = -1.20 \times 10^{-6}$ m/W, and $\chi_{3img} \approx 2.10 \times 10^{-14}$ m$^2$/V$^2$ ($\approx 1.5 \times 10^{-6}$ esu). Finally, based on Fig. 14 we consider the modulation depth of 25%, approximately.

We highlight that the nonlinear characterization of SWCNTs has been a special case in this work. However, the high power amplifier applications are not limited to the possibility of accomplishing the nonlinear characterization of other nanostructured materials deposited on the optical fiber end-face. It could have important applications in characterization of nonlinear effects in optical fibers, such as Raman effect, saturable absorbers, phase self-modulation, etc.

## 4. Conclusions

In this work, we have presented a high power pulsed erbium-doped fiber amplifier, which consists of two identical amplification stages in reflective configuration. Our experimental results show that using 20 kHz of frequency the output power of the amplifier can be set to a maximum peak power 41 W, with a gain of 43.1 dB,

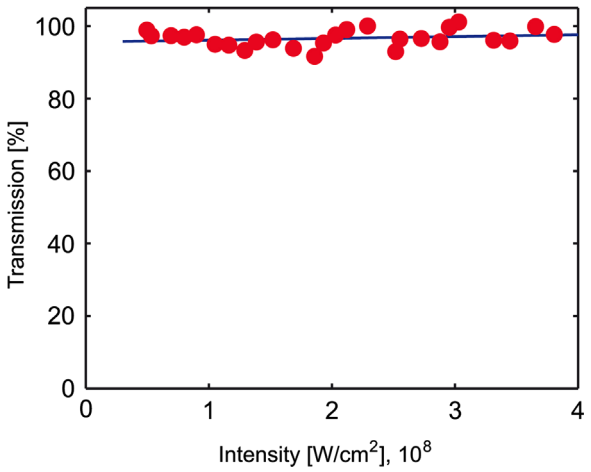


**Fig. 13.** Response to the optical transmittance of lacquer applied on optical fiber end-face.

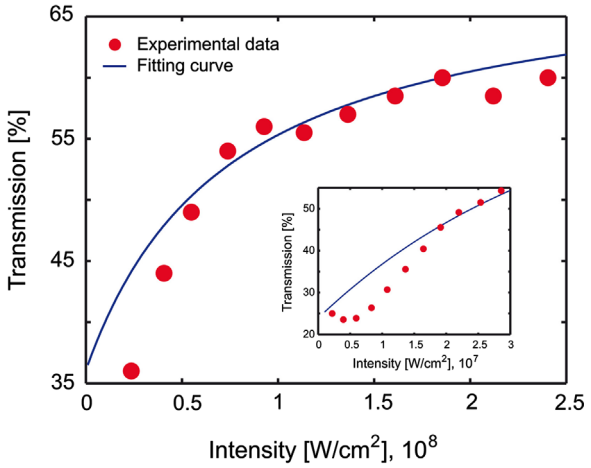


**Fig. 14.** Nonlinear characterization of SWCNTs with a thin-film of lacquer on optical fiber end-face.

approximately. However, it is possible to obtain a higher power if the frequency is lower than 20 kHz. The advantage of this high power amplifier is that the output power can be adjusted either by an attenuator limiting the signal path or through the temporal pulse duration. Additionally, this system uses a single optical pumping for both stages of amplification. Such characteristics allow us to consider that the high power amplifier system is inexpensive, it has a stable output, and it is easy to implement.

The high power amplifier can be applied to carry out the nonlinear characterization of nanomaterials deposited on optical fiber or nonlinear effects of optical fibers by means of the P-scan technique. We have demonstrated the nonlinear characterization of optical properties of SWCNTs deposited on the optical fiber end-face by photodeposition technique. We obtained a modulation depth of 25%, approximately. To our knowledge, this is the first report of nonlinear characterization of SWCNTs deposited on the optical fiber end-face by using the photodeposition technique. Based on the nonlinear characterization, we showed an application of the high power amplification system, and we consider that it can be very helpful in an important area of scientific research and development.

## Acknowledgements

This work was supported by CONACyT-Mexico through the project number 130983 as well as VIEP-BUAP under project 339.

## References

[1] Agrawal GP. Fiber-optic communications systems. 2nd ed.. New York: John Wiley and Sons; 1997.
[2] Song C, Xu W, Luo Z, Luo A, Chen W. Switchable and tunable dual-wavelength ultrashort pulse generation in a passively mode-locked erbium-doped fiber ring laser. Optics Communications 2009;282:4408–12.
[3] Pottiez O, Ibarra-Escamilla B, Kuzin EA. Large amplitude noise reduction in ultrashort pulse trains using a power-symmetric nonlinear optical loop mirror. Optics & Laser Technology 2009;41:384–91.
[4] Bello-Jiménez M, Kuzin EA, Ibarra-Escamilla B, Flores-Rosas A. Optimization of two-stage single-pump erbium-doped fiber amplifier with high amplification for low frequency nanoscale pulses. Optical Engineering 2007;46:1–6.
[5] Camas J, Mendoza S, Kuzin E, Pottiez O, García C, Vázquez R. High gain erbium-doped fiber amplifier for the investigation of nonlinear processes in fibers. Optical Fiber Technology 2008;14:237–41.
[6] Kataura H, Kumazawa Y, Maniwa Y, Umezu I, Susuki S, Ohtsuka Y, et al. Optical properties of single-well carbon nanotubes. Synthetic Metals 1999;103:2555–8.
[7] Ugawa A, Hwang J, Gommans HH, Tashiro H, Rinzler AG, Tanner DB. Far-infrared to visible optical conductivity of single-wall carbon nanotubes, Current Applied Physics, vol. 1;2001:45–9.
[8] Kampfrath T, von Volkmann K, Aguirre CM, Desjardins P, Martel R, Krenz M, et al. Mechanism of the far-infrared absorption of carbon-nanotube films. Physical Review Letters 2008;101:1–4.
[9] Nemilentsau AM, Slepyan GY, Khrutchinskii AA, Maksimenko SA. Third-order optical nonlinearity in single-wall carbon nanotubes, Journal of Physics: Conference Series, vol. 44;2006:2246–53.
[10] Wang J, Chen Y, Blau WJ. Carbon nanotubes and nanotube composites for nonlinear optical devices. Journal of Materials Chemistry 2009;19:7425–43.
[11] Harun SW, Ismail MA, Ahmad F, Ismail MF, Nor RM, Zulkepely NR, et al. A Q-switched erbium-doped fiber laser with a carbon nanotube based saturable absorber. Chinese Physics Letters 2012;29:1–3.
[12] Kivistö S, Hakulinen T, Kaskela A, Aitchison B, Brown DP. Carbon nanotube films for ultrafast broadband technology. Optics Express 2009;17:2358–63.
[13] Il'ichev NN, Obraztsova ED, Garnov SV, Mosaleva SE. Nonlinear transmission of single-wall carbon nanotubes in heavy water at a wavelength of 1.54 μm and self-mode locking in a Er:glass laser obtained using a passive nanotube switch. Quantum Electronics 2004;34:572–4.
[14] Rutherglen C, Jain D, Burke P. Nanotube electronics for radio frequency applications. Nature Nanotechnology 2009;4:811–9.
[15] Han H, Chen J, Diamant Y, Etienne M, Walser A, Dorsinville R, et al. Nonlinear transmission properties of nanostructures with single-wall carbon nanotubes and conductive polymers. Applied Physics Letters 2005;86:1–3.
[16] Yamashita S, Set SY, Goh CS, Kikuchi K. Ultrafast saturable absorbers based on carbon nanotubes and their applications to passively mode-locked fiber lasers. Electronics and Communications in Japan 2007;90:87–94.
[17] Ortega-Mendoza JG, Chávez F, Zaca-Morán P, Felipe C, Pérez-Sánchez GF, Beltran-Pérez G, et al. Selective photodeposition of zinc nanoparticles on the core of a single-mode optical fiber. Optics Express 2013;21:6509–18.
[18] Lamarre JM, Billard F, Harkati C, Lequime M, Roorda S, Martinu L. Anisotropic nonlinear optical absorption of gold nanorods in a silica matrix. Optics Communications 2008;281:331–40.
[19] Lami JF, Hirlimann C. Two-photon excited room-temperature luminescence of CdS in the femtosecond regime. Physical Review B 1999;60:4763–70.